RASĀYAN *J. Chem.*
Vol. 19 | No. 1 | 646-651 | January-March | 2026
ISSN: 0974-1496 | e-ISSN: 0976-0083 | CODEN: RJCABP
http://www.rasayanjournal.com
http://www.rasayanjournal.co.in

SUPERIOR ANTIBACTERIAL FEATURES OF ZnO NANOPARTICLES PREPARED BY *Azadirachta indica:* MEDIATED GREEN SYNTHESIS ROUTE

S. Ghadai[1], Suchismita Acharya[1,✉], M. Sahoo[2], M. P. Mishra[2], S. K. Biswal[1], and S. N. Sarangi[3]

[1]School of Applied Sciences, Centurion University of Technology and Management, Odisha, India

[2]School of Paramedics and Allied Health Sciences, Centurion University of Technology and Management, Bhubaneswar, Odisha, India

[3]Institute of Physics, Bhubaneswar, Odisha, India

✉Corresponding author: suchismita.acharya@cutm.ac.in

ABSTRACT

Zinc oxide nanoparticles exhibit size- and morphology-dependent properties strongly influenced by synthesis routes. We report ZnO nanoparticles prepared via chemical co-precipitation [ZnO(C)] and a green route using *Azadirachta indica* leaf extract [ZnO(G)]. Furthermore, their structure–property correlations have been systematically studied by several characterization methods. Formation of a hexagonal wurtzite ZnO phase was confirmed by X-ray diffraction analysis, revealing that ZnO(G) possessed comparatively smaller crystallite sizes, a result of the controlled nucleation and growth imparted by phytochemicals present in the Azadirachta indica extract. FESEM analysis revealed irregular agglomerates in ZnO(C), whereas ZnO(G) exhibited uniform spherical structures. UV–Vis spectra showed strong near-UV absorption, with band gaps of ~3.60 eV (ZnO(C)) and ~3.63 eV (ZnO(G)), the latter slightly redshifted by defect states and biomolecule interactions. Antibacterial tests against *Escherichia coli* (*E. coli*) and *Staphylococcus aureus* (*S. aureus*) showed stronger inhibition for ZnO(G), attributed to residual phytoconstituents and altered surface chemistry. Overall, synthesis pathways dictate crystallite size, morphology, optical bandgap, and antimicrobial activity, highlighting *Azadirachta indica*-mediated green synthesis as a sustainable route to prepare nano ZnO for biomedical use.

Keywords: ZnO, Nanoparticle, Green Synthesis, Co-Precipitation Method, Antibacterial Property, Phytochemicals.

RASĀYAN *J. Chem.*, Vol. 19, No.1, 2026

INTRODUCTION

The unique physical, chemical, and functional features of nanomaterials have made them a major focus of scientific research over the last few decades.[1,2] They are extensively investigated for applications in environmental remediation, optoelectronics, catalysis, energy storage, and biomedicine, with emphasis on correlating nanoscale structural parameters with performance.[2,3,4,5] Among nanomaterials, metal oxide nanoparticles are notable for their abundance, stability, tunable electronic structure, and versatile synthesis strategies that allow control over size, shape, and crystallinity.[6] Belonging to the II–VI semiconductor family, zinc oxide (ZnO) has received extensive research attention owing to its exceptional functional characteristics and wide range of applications.[7,8] It primarily crystallizes in the hexagonal wurtzite structure, featuring a direct wide bandgap of approximately 3.2–3.4 eV and a high excitonic binding energy of around 60 meV.[9,10] These structural and electronic features make ZnO highly favourable for optical and electronic applications.[9,10] Defect chemistry involving oxygen vacancies and zinc interstitials further makes ZnO suitable for optoelectronic devices, sensors, photocatalysts, and antimicrobial coatings.[10,11,12] Its biocompatibility and relatively low toxicity enhance its biomedical potential in wound healing, antibacterial dressings, and drug delivery.[9] The wide bandgap also ensures strong ultraviolet absorption, enabling use in sunscreens, UV detectors, and transparent conductive films.[9,10] ZnO nanoparticles are also effective antibacterial agents, where ROS generation, surface defects, and zinc ion release act synergistically.[13] ZnO properties strongly depend on the synthesis route, which

dictates crystallite size, morphology, surface area, and defect density.[14] Nanoparticles of ZnO are being fabricated using different methods like hydrothermal processing, sol–gel routes, microwave-assisted reactions, and precipitation techniques. Of these, the chemical co-precipitation approach is particularly attractive because it combines simplicity and large-scale applicability with the advantage of producing crystalline ZnO under mild temperature conditions.[9,15] Co-precipitation involves reacting zinc salts with alkaline agents to form hydroxide intermediates, later calcined to ZnO. The green synthesis approach has emerged as a sustainable and environmentally friendly alternative[16], where phytochemicals (flavonoids, terpenoids, polyphenols, alkaloids) serve as stabilizing and reducing agents, eliminating harsh chemicals.[17] Plant extracts from *Artemisia*, *Allium cepa*, *Sargassum* species, and neem (*Azadirachta indica*) have successfully yielded ZnO nanoparticles with controlled morphologies and enhanced functionalities.[18] Bioactive molecules not only guide nucleation and growth but also impart additional antimicrobial properties. Compared with chemical routes, green synthesis minimizes toxic byproducts, lowers energy use, and improves biocompatibility, making it attractive for biomedical and environmental use. This study aims to establish structure–property correlations in ZnO nanoparticles synthesized via chemical co-precipitation and *A. indica*-mediated green synthesis. While co-precipitation ensures reproducibility and crystallinity, green synthesis offers phytochemical-mediated morphology control and eco-friendliness. Despite progress, comparative studies linking the synthesis route to structure, morphology, bandgap, and antibacterial activity remain limited. To address this, we report ZnO nanoparticles prepared by both methods and evaluate their performance in inhibiting the bacterial growth (*E. coli* and *S. aureus*). Results showed synthesis pathways significantly influence crystallite size, morphology, optical transitions, and antimicrobial efficacy, underscoring the importance of synthesis–structure–property correlations for optimizing ZnO in advanced materials and biomedical applications. Overall, the findings highlight the potential of green synthesis as a sustainable route for tailoring ZnO nanoparticles with superior multifunctional properties.

EXPERIMENTAL

Material and Methods

ZnO nanoparticles were synthesized using two distinct approaches: chemical co-precipitation and green synthesis. In the co-precipitation method, 0.5 M zinc acetate dihydrate was dissolved in 100 mL of distilled water and stirred continuously at room temperature. To this solution, 0.2 M ammonium hydroxide was added dropwise until the pH reached approximately 10, resulting in the formation of zinc hydroxide ($Zn(OH)_2$) precipitate.

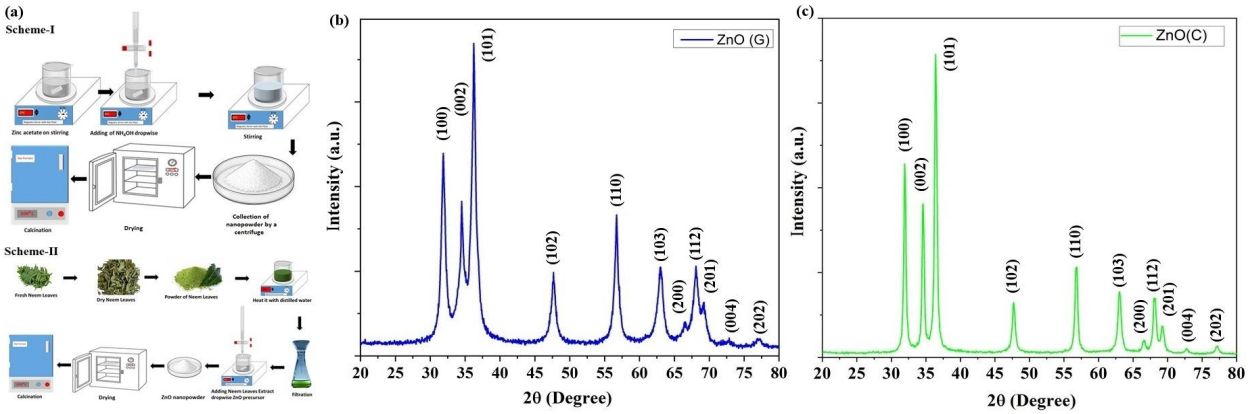

Fig.-1: (a) Schematic Illustration of the Synthesis Process, and XRD Spectra of ZnO Prepared by Co-precipitation (b) and Green Synthesis (c) Methods

The reaction mixture was stirred for 3 hours and then allowed to age for 24 hours. Impurities were eliminated by repeatedly rinsing the obtained precipitate with distilled water and ethanol. After the washing process, the sample was dried in an oven at 100 °C for 12 hours to ensure complete moisture removal. The dried product was subsequently calcined at 300 °C for 2 hours to produce phase-pure ZnO nanoparticles with good crystallinity and uniform particle size. In the green synthesis approach, the

extract from *Azadirachta indica* (neem) leaves functioned simultaneously as a reducing and stabilizing medium. To prepare the extract, 20 g of finely chopped leaves were boiled in 100 mL of distilled water for 20 minutes, after which the mixture was allowed to cool and was subsequently filtered to obtain a clear solution. To this extract, a 0.5 M zinc acetate solution was added under constant stirring, and the pH was adjusted to around 10 using 0.2 M sodium hydroxide to initiate nanoparticle formation. The reaction mixture was stirred for 2–3 hours and left to age for 24 hours. The resulting precipitate was washed thoroughly with water and ethanol, dried at 100 °C for 12 hours, and calcined at 300 °C for 2 hours to obtain crystalline ZnO nanoparticles. The overall synthesis procedure is illustrated schematically in Fig.-1.

RESULTS AND DISCUSSION

XRD spectra of ZnO nanoparticles synthesized by the two routes are shown in Fig.-1 (b and c). Both samples exhibited distinct diffraction peaks at 2θ values corresponding to different characteristic planes of hexagonal wurtzite ZnO with space group $P6_3$ mc.[19–22] Sharp, intense peaks confirmed good crystallinity, though differences in peak broadening indicated variations in crystallite size and lattice strain. Debye–Scherrer analysis showed a larger crystallite size for ZnO(C) (35.21 nm) compared to ZnO(G) (21.28 nm), attributed to slower nucleation and growth kinetics in the phytochemical-mediated green synthesis.[21,22] ZnO(C) exhibited slightly higher microstrain, whereas ZnO(G) showed lower microstrain and dislocation density, signifying better crystalline quality. This improvement arises from phytochemicals in *Azadirachta indica* extract acting as stabilizing and capping agents, reducing stress and defect formation during growth.[23,24] The unit cell volume (Table-1) was consistent with the wurtzite structure and showed negligible variation, confirming structural stability. Thus, while both methods produced phase-pure ZnO, co-precipitation yielded larger crystallites with higher strain and defects, whereas green synthesis generated smaller, defect-controlled crystallites, advantageous for surface-active and defect-mediated applications.

Table-1: Structural Parameters of ZnO Samples Estimated from XRD Results

Sample	Size	Strain	Lattice parameter		Dislocation density	Unit cell volume
			a (Å)	*c* (Å)	$\delta = 1/D^2$ (nm^{-2})	($V=a^2c$) ($Å)^3$
ZnO(C)	35.21	0.0047	3.203	5.187	8.06×10^{-4}	50.22
ZnO(G)	21.28	0.0012	3.182	5.173	3.87×10^{-4}	51.37

The surface morphology of ZnO nanoparticles synthesized by co-precipitation and green synthesis was examined using SEM, with representative images shown in Fig.-2. Images (a and b) correspond to ZnO(C), while (c and d) represent ZnO(G). Clear morphological differences were observed, reflecting the impact of chemical versus phytochemical-mediated growth.[23] ZnO(C) displayed larger grain-like structures with irregular semi-spherical morphology and noticeable agglomeration (Fig.-2a), attributed to the high surface energy of nanosized ZnO promoting coalescence during synthesis and calcination. The crystalline domains observed align with the sharp XRD peaks, as co-precipitation favoured nucleation and particle growth, yielding larger crystallites with reduced surface roughness.[25]

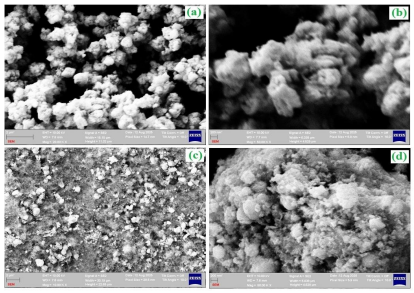

Fig.-2: FESEM Images ZnO Prepared by Co-precipitation (a and b) and Green Synthesis (c and d) Methods

By contrast, ZnO(G) exhibited more uniform, quasi-spherical nanoparticles with smaller sizes and better dispersion, though some agglomeration remained typical of oxide nanoparticles. The use of *Azadirachta indica* extract restricted excessive growth through the stabilizing and capping actions of phytochemicals.[24] These biomolecules acted as reducing agents and provided steric hindrance, producing

finer, porous nanostructures.[23,24] Such smaller, well-dispersed particles with higher surface area are advantageous for catalysis and antibacterial activity.

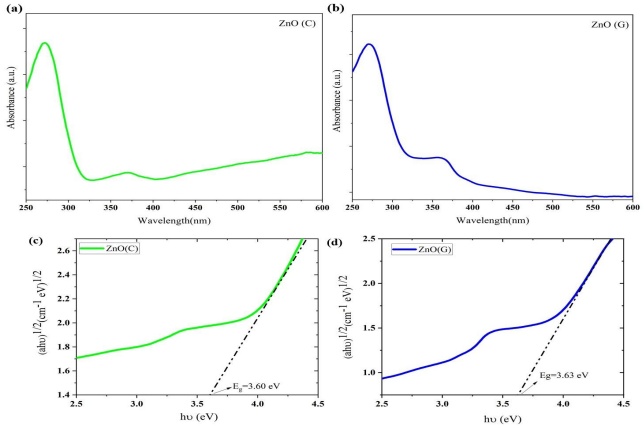

Fig.-3: UV-Vis Spectra (a and b) and Tauc's Plots (c and d) of ZnO Samples

Figure-3 (a and b) depicts the optical absorption patterns of ZnO(C) and ZnO(G), both exhibiting strong UV absorption due to the wide band gap and semiconducting nature of ZnO.[24,26] The high UV absorption intensity confirms their strong optical activity, making them suitable for photocatalysis, UV shielding, and optoelectronic applications. The determination of the optical band gap (Eg) was carried out from Tauc's plot (Fig.-3c and d), where the straight-line portion of the $(\alpha h\nu)^2$ vs. hν graph was extrapolated to obtain the value.[27] Band gap values were 3.60 eV for ZnO(C) and 3.63 eV for ZnO(G), both higher than bulk ZnO (3.37 eV), attributed to quantum confinement effects at the nanoscale.[28] The slightly larger Eg of ZnO(G) suggests a smaller particle size and stronger confinement, consistent with SEM results. Additionally, phytochemicals in the green synthesis may induce surface passivation, altering the electronic structure and widening the band gap.[23,24] Thus, UV–Vis and Tauc's analyses confirm that both synthesis routes produce ZnO nanoparticles with excellent optical properties, with subtle differences linked to synthesis conditions. To determine their antibacterial potential, the synthesized ZnO nanoparticles were tested against two model bacterial species: *S. aureus* and *E. coli*. Zone of inhibition (ZOI) results (Fig.-4a-d) showed ZnO(C) with 15.2 ± 0.01 mm (*E. coli*) and 12.6 ± 0.03 mm (*S. aureus*), while ZnO(G) exhibited significantly larger zones of 18.1 ± 0.03 mm and 17.0 ± 0.02 mm, respectively.

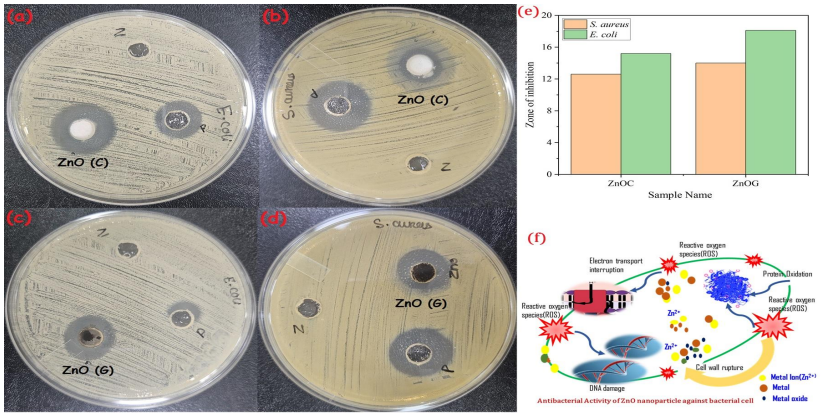

Fig.-4: Zone of Inhibition (a-d), its Variation (e) and Mechanism of Antibacterial Action (f) of ZnO Samples for *E. coli* and *S. aureus*

Figure-4(e) illustrates these variations, confirming the superior antibacterial efficiency of green-synthesized ZnO over chemically synthesized ones.[22–24] The enhanced activity of ZnO(G) is attributed to phytochemicals from *Azadirachta indica* (flavonoids, terpenoids, alkaloids) acting synergistically with ZnO[22,23], smaller particle size and higher surface area, and better dispersion due to neem-derived biomolecules.[22–24] Antibacterial action involves ROS generation (·OH, O_2^-, H_2O_2), inducing oxidative stress, membrane damage, protein alteration, and DNA fragmentation.[22–24, 29] Additionally, Zn^{2+} ions disrupt enzyme functions and metabolic processes. Figure-4f schematically represents this mechanism.

While *E. coli* typically shows greater resistance due to its outer membrane, ZnO(G) displayed nearly comparable inhibition for both strains, demonstrating broad-spectrum potential. Overall, green-synthesized ZnO retained intrinsic antimicrobial features and gained added effectiveness from plant-mediated functionalization, making it highly suitable for biomedical and environmental applications.

CONCLUSION

ZnO nanoparticles were synthesized via chemical co-precipitation and *Azadirachta indica*-mediated green synthesis to evaluate how synthesis pathways influence their structural, morphological, optical, and antibacterial behaviour. XRD confirmed phase-pure wurtzite ZnO in both cases, with ZnO(G) showing a smaller crystallite size, lower microstrain, and reduced dislocation density, indicating superior crystalline quality over ZnO(C). SEM observations supported this, revealing larger, agglomerated ZnO(C) particles versus smaller, quasi-spherical, well-dispersed ZnO(G), attributed to neem-derived phytochemicals. UV–Vis analysis showed strong UV absorption, with band gaps of 3.60 eV (ZnO(C)) and 3.63 eV (ZnO(G)), the latter linked to finer particle size and surface passivation by phytochemicals. Antibacterial assays against the bacterial strains demonstrated stronger activity of green-synthesized ZnO, evidenced by larger inhibition zones. Enhanced performance is attributed to a smaller size, higher surface reactivity, and bioactive compounds that promote ROS generation and Zn^{2+} ion release, causing bacterial membrane and intracellular damage. Overall, green synthesis offers an eco-friendly route that improves structural integrity, optical behaviour, and antibacterial efficacy, highlighting the potential of *A. indica*-mediated ZnO as multifunctional nanomaterials for biomedical applications, ensuring good health and well-being.

CONFLICT OF INTERESTS

The authors declare that there is no conflict of interest.

AUTHOR CONTRIBUTIONS

The present work is related to *SDG-3: Good Health and Well-Being*. All the authors contributed significantly to this manuscript, participated in reviewing/editing and approved the final draft for publication. The research profile of the authors can be verified from their ORCID ids, given below:

S. Ghadai https://orcid.org/0009-0005-6841-8379
S. Acharya https://orcid.org/0000-0001-7867-2462
M. Sahoo https://orcid.org/0009-0005-0839-5312
M. P. Mishra https://orcid.org/0000-0002-8548-1784
S. K. Biswal https://orcid.org/0000-0003-0460-2562
S. N. Sarangi https://orcid.org/0000-0001-9273-4981

Cite this article as: S. Ghadai *et al.*, *Rasayan J. Chem.*, 19(1), 646-651(2026), https://doi.org/10.31788/RJC.2026.1919571.

REFERENCES

1. B. Mekuye and B. Abera, *Nano Select*, **4(8)**, 486(2023), https://doi.org/10.1002/nano.202300038
2. S. A. Ahire, A. A. Bachhav, T. B. Pawar, B. S. Jagdale, A. V. Patil and P. B. Koli, *Results in Chemistry*, **4**, 100633(2022), https://doi.org/10.1016/j.rechem.2022.100633
3. S. Aththanayaka, G. Thiripuranathar and S. Ekanayake, *Materials Today Sustainability*, **20**, 100206(2022), https://doi.org/10.1016/j.mtsust.2022.100206
4. K. J. Hughes, M. Ganesan, R. Tenchov, K. A. Iyer, K. Ralhan, L. L. Diaz, R. E. Bird, J. Ivanov and Q. A. Zhou, *ACS Omega*, **10(8)**, 7530(2025), https://doi.org/10.1021/acsomega.4c10929
5. V. Takhar and S. Singh, *Environmental Science: Nano*, **12**, 2516(2025), https://doi.org/10.1039/D5EN00049A
6. M. S. Chavali and M. P. Nikolova, *SN Applied Sciences*, **1**, 607(2019), https://doi.org/10.1007/s42452-019-0592-3

7. D. Buckley, A. Lonergan and C. O'Dwyer, *ECS Journal of Solid State Science and Technology*, **14(1)**, 015001(2025), https://doi.org/10.1149/2162-8777/ada3a2
8. R. Hashim, S. P. S., A. K. K. Ali, S. John, C. M. Sam, V. R. and K. S. G., *Materials Research Innovations*, 1(2025), https://doi.org/10.1080/14328917.2025.2487928
9. N.R. Panda, B.S. Acharya, P. Nayak, and B.P. Bag, *Ultrasonics Sonochemistry*, **21(2)**, 582(2014), https://doi.org/10.1016/j.ultsonch.2013.08.007
10. N.R. Panda, B.S. Acharya, and P. Nayak, *Journal of Materials Science: Materials in Electronics,* **24**, 4043(2013), https://doi.org/10.1007/s10854-013-1359-z
11. W.Amananti and A. B. Riyanta, *Rasayan Journal of Chemistry*, **18(4)**, 2249(2025), http://doi.org/10.31788/RJC.2025.1849377
12. A. Singhal, G. P. Meghwal, A. Kumari, N. Fahmi, R.V. Singh, P. Meena and R. Meena, *Rasayan Journal of Chemistry*, **18(1)**, 325(2025), http://doi.org/10.31788/RJC.2025.1819211
13. A. M. Mohammed, M. Mohammed, J. K. Oleiwi, F. H. Ihmedee, T. Adam, B. O. Betar and S. C. B. Gopinath, *Nano Trends*, **11**, 100145(2025), https://doi.org/10.1016/j.nwnano.2025.100145
14. A.Kistan, P. Mahimairaj, S. Mohan, R. Jeevalatha, P. Sivakumar, *Rasayan Journal of Chemistry*, **19(1)**, 575(2026), http://doi.org/10.31788/RJC.2026.1919577
15. R. E. Adam, G. Pozina, M. Willander and O. Nur, *Photonics and Nanostructures: Fundamentals and Applications*, **32**, 11(2018), https://doi.org/10.1016/j.photonics.2018.08.005
16. I. S. Afonso, B. Cardoso, G. Nobrega, G. Minas, J. E. Ribeiro and R. A. Lima, *Journal of Environmental Chemical Engineering*, **12(5)**, 114022(2024), https://doi.org/10.1016/j.jece.2024.114022
17. G. I. Edo, A. N. Mafe, A. B. M. Ali, P. O. Akpoghelie, E. Yousif, E. F. Isoje, U. A. Igbuku, K. Zainulabdeen, J. O. Owheruo, A. E. A. Essaghah, H. Umar, D. S. Ahmed and A. A. Alamiery, *Nano Translational Medicine*, **4**, 100080(2025), https://doi.org/10.1016/j.ntm.2025.100080
18. M. Y. Al-darwesh, S. S. Ibrahim and M. A. Mohammed, *Results in Chemistry*, **7**, 101368(2024), https://doi.org/10.1016/j.rechem.2024.101368
19. M. M. Almoneef, M. A. Awad, H. H. Aldosari, A. A. Hendi, H. A. Aldehish, N. M. Merghani and S. G. Alshammari, *Heliyon*, 10(12), e32714 (2024), https://doi.org/10.1016/j.heliyon.2024.e32714
20. A. Sobha, J. Johnson, K. P. Abhina, *Journal of Alloys and Compounds*, **1037**, 182365(2025), https://doi.org/10.1016/j.jallcom.2025.182365
21. S. Faisal, H. Jan, S. A. Shah, S. Shah, A. Khan, M. T. Akbar, M. Rizwan, F. Jan, N. Akhtar, A. Khattak and S. Syed, *ACS Omega*, **6(14)**, 9709(2021), https://doi.org/10.1021/acsomega.1c00310
22. A. Halder, G. R. Mohan, S. Matheshwaran and S. K. Jha, *Next Materials*, **8**, 100725(2025), https://doi.org/10.1016/j.nxmate.2025.100725
23. G. Joesna, A. Alodhayb, P. Sasikumar, T. L. Sree, R. Z. Ferin, D. Sankar, A. Prabakaran, M. Prasath, M. M. Muthuramamoorthy, M. G. Mohamed and M. Vimalan, *Chemical Physics Impact*, **10**, 100821(2025), https://doi.org/10.1016/j.chphi.2025.100821
24. E. Tsegahun and M. Aklilu, *Discover Nano*, **20**, 145(2025), https://doi.org/10.1186/s11671-025-04260-4
25. I. O. Ali, H. Nady, M. I. Mohamed and T. M. Salama, *Journal of the Indian Chemical Society*, **101(12)**, 101480(2024), https://doi.org/10.1016/j.jics.2024.101480
26. M. R. Ahmad, A. A. Ansari, M. Dhayal and R. Lv, *Renewable and Sustainable Energy Reviews*, **219**, 115767(2025), https://doi.org/10.1016/j.rser.2025.115767
27. J. Josun, P. Sharma and V. K. Garg, *Results in Optics*, **14**, 100601(2024), https://doi.org/10.1016/j.rio.2023.100601
28. R. Torkamani and B. Aslibeiki, *Journal of Crystal Growth*, **618**, 127317(2023), https://doi.org/10.1016/j.jcrysgro.2023.127317
29. S. Acharya, and D. Sahu, *Rasayan Journal of Chemistry*, **16(4)**, 2280(2023), https://doi.org/10.31788/RJC.2023.1648647

[RJC-9571/2025]